

# Thermoelectric response of a hot and weakly magnetized anisotropic QCD medium

Salman Ahamad Khan\*, Debarshi Dey† and Binoy Krishna Patra‡

Department of Physics,  
Indian Institute of Technology Roorkee, Roorkee 247667, India

September 19, 2023

## Abstract

We have studied the Seebeck and Nernst coefficients of a weakly magnetized hot QCD medium having a weak momentum anisotropy within the kinetic theory approach. The thermal medium effects have been incorporated in the framework of a quasi-particle model where the medium dependent mass of the quark has been calculated using perturbative thermal QCD in the presence of a weak magnetic field which leads to different masses for the left ( $L$ ) and right ( $R$ ) handed chiral quark modes. We have found that the Seebeck and Nernst coefficient magnitudes for the individual quark flavors as well as for the composite medium are decreasing functions of temperature and decreasing functions of anisotropy strength. The Nernst coefficient magnitudes are about an order of magnitude smaller than their Seebeck counterparts, indicating the Seebeck effect constitutes a stronger response than the Nernst effect. The average percentage change corresponding to switching between quasiparticle modes ( $L \rightarrow R$  or  $R \rightarrow L$ ) is an order of magnitude smaller for Nernst coefficients, compared to the Seebeck coefficients.

## I Introduction

Heavy ion collisions at ultra-relativistic energies give rise to a state of matter comprising of asymptotically free quarks and gluons-the Quark Gluon Plasma (QGP). Several observables are considered as signatures of creation of such a medium; this includes photon and dilepton spectra[1, 2], quarkonium suppression[3–5], elliptic flow[6, 7], jet quenching[8–10], etc. Experimentally, significant evidence now exists of the observation of these signals, and thus, of the creation of QGP matter in Ultrarelativistic Heavy Ion collisions (URHICs)

---

\*skhan@ph.iitr.ac.in

†ddey@ph.iitr.ac.in, debs.mvm@gmail.com

‡binoy@ph.iitr.ac.in

at experimental facilities such as the Brookhaven National Laboratory Relativistic Heavy Ion Collider (RHIC) [11–13] and Large Hadron Collider (LHC)[14, 15]. Right after the formation of QGP, it expands and cools and transitions into a mildly interacting collection of hadrons. At very small baryon chemical potentials ( $\mu_B \sim 0$ ), with massive quarks, the results of lattice QCD indicate that the transition is actually an analytic crossover rather than a true phase transition. [16–19]. The sign problem of lattice QCD at finite  $\mu_B$  makes it an unreliable tool to explore large parts of the QCD phase diagram[20, 21].

The QGP lives for a very short period of time and does not expand at the same rate in all the directions. The colliding nuclei are Lorentz contracted due to their relativistic speeds. The overlap volume of such nuclei in a non-central collision is anisotropic in the plane perpendicular to the beam (transverse plane). This spatial asymmetry in coordinate space gets converted into an opposite asymmetry in the momentum space which is ultimately reflected in the hadron  $p_T$  spectra. A convenient way of taking into account the anisotropy of the medium was introduced by Romatschke and Strickland wherein the anisotropic distribution function is obtained from an arbitrary isotropic one by the rescaling of only one direction in momentum space, *i.e.* by stretching or squeezing the isotropic distribution function of the medium constituents (partons)[22]. This parametrisation of the anisotropy involving a single direction and a single anisotropy parameter,  $\xi$  (spheroidal momentum anisotropy), was used to calculate the collective modes of finite temperature QCD and study their impact in thermalization of the QGP medium[22–25]. Hard loop effective theories have also been used to study anisotropy; its equivalence with the kinetic theory approach was shown by Mrówczyński and Thoma, wherein they calculated the self-energies and dispersion relations for QGP partons[26]. Existence of instabilities associated with gluon collective modes in an anisotropic QGP has been observed and their growth rates have also been calculated[27, 28]. This description has also been used to study photon and dilepton production from the QGP [29, 30], the QGP heavy quark potential [31], and bottomonia suppression[32]. In addition to the case of spheroidal anisotropy, ellipsoidal momentum anisotropy has also been considered, which is characterised by two or more independent anisotropic parameters. In particular, parton self energies have been calculated in an ellipsoidally anisotropic QGP[33]. Anisotropic momentum distributions have also been used in relativistic hydrodynamic models to study the evolution of QGP to hadrons[34–38]. In fact, anisotropic hydrodynamics (aHydro) has been more accurate than its isotropic counterpart in the description of non-equilibrium dynamics[39–44]. As such, transport coefficients like electrical conductivity[45], heavy quark drag and diffusion coefficients[46] have also been evaluated in an anisotropic plasma.

Apart from causing an anisotropic expansion of the created matter, non-central heavy ion collisions also lead to creation of large magnetic fields[47]. These magnetic fields, produced mainly by the spectator protons moving away from each other at relativistic

speeds, reach magnitudes upto  $eB \sim 10^{-1}m_\pi^2 (\simeq 10^{17} \text{ Gauss})$  for SPS energies,  $eB \sim m_\pi^2$  for RHIC energies and  $eB \sim 15m_\pi^2$  for LHC energies[48]. The decay rate of the magnetic field depends strongly on the electrical conductivity of the medium which is exposed to the field[49–58]. Depending on the strength of the background magnetic field, several interesting phenomena of the created matter can be probed. A strong background magnetic field causes separation of charges in a chiral QGP medium leading to a magnetic field dependent current, which is non-Maxwellian and has no analog in classical physics. This is the Chiral Magnetic effect[59–61]. Other phenomena induced by strong magnetic fields include magnetic catalysis[62], chiral magnetic wave[63], axial magnetic effect[64, 65], etc. A small electrical conductivity, however, would lead to only a small fraction of the initial magnetic field surviving when the created matter thermalizes. This has motivated several studies where the background magnetic field is considered to be weak. Further, such a weak field can give rise to novel phenomenological results like the lifting of mass degeneracy between the left and right handed quark effective masses[66]. Transport phenomena in the presence of weak magnetic field has been under investigation in the recent past[67–72]

In this article, we study for the first time, the thermoelectric response of an anisotropic QGP medium in the presence of a weak magnetic field, by incorporating the non-degenerate left and right chiral quasiparticle masses of quarks. Fluctuations in the initial energy density of heavy-ion collisions can create large temperature differences between the central and peripheral regions of the fireball[73]. This, coupled with a finite chemical potential can potentially give rise to thermoelectric phenomena: Seebeck and Nernst effects. The ability to convert a temperature gradient into an electric field is quantified by the Seebeck and Nernst coefficients. Thermoelectric phenomena have been previously investigated both in the presence and absence of magnetic field in a thermal QCD medium[74–80].

In what follows, we present the calculation of the thermoelectric coefficients of a QGP medium, taking into account the expansion induced anisotropy of the momentum distribution of the partons, in the presence of a weak background magnetic field. The paper is organized as follows: In section II the quasiparticle model used in this work is described. In section III, the calculation of Seebeck and Nernst coefficients are outlined both for single component and multi component mediums. In section IV, the results are plotted and their interpretations discussed. Finally, we conclude in section V.

## II Quasiparticle model

The central feature of quasi particle models is that a strongly interacting system of massless quarks and gluons can be described in terms of massive, weakly interacting quasi-

particles originating due to the collective excitations. There are many quasi-particle models such as Nambu-Jona-Lasinio (NJL) model and PNJL model [81–84] which are based on the respective effective QCD models, effective fugacity model [85] and the recently proposed quasi-particle model based on the Gribov–Zwanziger quantization [86–88]. In this study, we have used quasi-particle model [89] which has only a single adjustable parameter and the medium effects enter through the dispersion relations of the quark and gluon quasi-particles. The temperature and magnetic field-dependent masses of the quarks and gluons have been computed from the poles of their resummed propagators obtained from Dyson-Schwinger equations. The respective self-energies have been calculated using perturbative thermal QCD in a strong magnetic field background. The quasi particle mass of the  $i^{\text{th}}$  flavor is written phenomenologically as [89]

$$m_i^2 = m_{i,0}^2 + \sqrt{2}m_{i,0}m_{i,T} + m_{i,T}^2, \quad (1)$$

where  $m_{i,0}$  and  $m_{i,T}$  are the current quark mass and medium generated quark mass.  $m_{i,T}$  has been calculated using the HTL perturbation theory as [90, 91]

$$m_{i,T}^2 = \frac{g'^2 T^2}{6} \left( 1 + \frac{\mu^2}{\pi^2 T^2} \right), \quad (2)$$

where  $g' = \sqrt{4\pi\alpha_s}$  refers to the coupling constant which depends on the temperature as

$$\alpha_s(T) = \frac{g'^2}{4\pi} = \frac{6\pi}{(33 - 2N_f) \ln \left( \frac{Q}{\Lambda_{QCD}} \right)}, \quad (3)$$

where,  $Q$  is set at  $2\pi\sqrt{T^2 + \frac{\mu^2}{\pi^2}}$ .

In the presence of a strong magnetic field, the coupling constant  $g = \sqrt{4\pi\alpha_s}$  runs with the temperature, chemical potential and magnetic field as [92]

$$\alpha_s(\Lambda^2, eB) = \frac{g^2}{4\pi} = \frac{\alpha_s(\Lambda^2)}{1 + b_1\alpha_s(\Lambda^2) \ln \left( \frac{\Lambda^2}{\Lambda^2 + eB} \right)}, \quad (4)$$

with

$$\alpha_s(\Lambda^2) = \frac{1}{b_1 \ln \left( \frac{\Lambda^2}{\Lambda_{\overline{MS}}^2} \right)}, \quad (5)$$

where  $\Lambda$  is set at  $2\pi\sqrt{T^2 + \frac{\mu^2}{\pi^2}}$  for quarks,  $b_1 = \frac{11N_c - 2N_f}{12\pi}$  and  $\Lambda_{\overline{MS}} = 0.176$  GeV.

Similarly the effective quark mass for  $i^{\text{th}}$  flavor in the case of a weak magnetic field can be parameterized like in the earlier cases as

$$m_{i,w}^2 = m_{i,0}^2 + \sqrt{2}m_{i,0}m_{i,L/R} + m_{i,L/R}^2, \quad (6)$$

where  $m_{i,L/R}$  refers to the thermal mass for the left- or right-handed chiral mode of  $i^{th}$  flavor which can be evaluated from the Dyson-Schwinger equation in weak magnetic field

$$S^{*-1}(P) = \not{P} - \Sigma(P). \quad (7)$$

$\Sigma(P)$  is the quark self energy in the weakly magnetized thermal medium. The general structure of quark self energy in the covariant form at finite temperature and magnetic field can be written as [66]

$$\Sigma(P) = -A'\not{P} - B'\not{\psi} - C'\gamma_5\not{\psi} - D'\gamma_5\not{b}, \quad (8)$$

where  $A', B', C', D'$  are the structure functions which can be evaluated by taking the appropriate contractions of Eqn. (8) as [66]

$$A'(p_0, p_\perp, p_z) = \frac{1}{4} \frac{\text{Tr}(\Sigma(P)\not{P}) - (P.u)\text{Tr}(\Sigma(P)\not{\psi})}{(P.u)^2 - P^2}, \quad (9)$$

$$B'(p_0, p_\perp, p_z) = \frac{1}{4} \frac{(-P.u)\text{Tr}(\Sigma(P)\not{P}) + P^2\text{Tr}(\Sigma(P)\not{\psi})}{(P.u)^2 - P^2}, \quad (10)$$

$$C'(p_0, p_\perp, p_z) = -\frac{1}{4}\text{Tr}(\gamma_5\Sigma(P)\not{\psi}), \quad (11)$$

$$D'(p_0, p_\perp, p_z) = \frac{1}{4}\text{Tr}(\gamma_5\Sigma(P)\not{b}). \quad (12)$$

The explicit form of the above structure functions have been calculated as [66]

$$A'(p_0, |\mathbf{p}|) = \frac{m_{th}^2}{|\mathbf{p}|^2} Q_1\left(\frac{p_0}{|\mathbf{p}|}\right), \quad (13)$$

$$B'(p_0, |\mathbf{p}|) = -\frac{m_{th}^2}{|\mathbf{p}|} \left[ \frac{p_0}{|\mathbf{p}|} Q_1\left(\frac{p_0}{|\mathbf{p}|}\right) - Q_0\left(\frac{p_0}{|\mathbf{p}|}\right) \right], \quad (14)$$

$$C'(p_0, |\mathbf{p}|) = -4g^2 C_F M^2 \frac{p_z}{|\mathbf{p}|^2} Q_1\left(\frac{p_0}{|\mathbf{p}|}\right), \quad (15)$$

$$D'(p_0, |\mathbf{p}|) = -4g^2 C_F M^2 \frac{1}{|\mathbf{p}|} Q_0\left(\frac{p_0}{|\mathbf{p}|}\right), \quad (16)$$

where

$$M^2(T, \mu, B) = \frac{|q_i B|}{16\pi^2} \left( \frac{\pi T}{2m_{i0}} - \ln 2 + \frac{7\mu^2 \zeta(3)}{8\pi^2 T^2} \right), \quad (17)$$

where  $\zeta$  corresponds to the Riemann zeta function.  $Q_0$  and  $Q_1$  refer to the Legendre functions of first and second kind, respectively, which are given by

$$Q_0(x) = \frac{1}{2} \ln\left(\frac{x+1}{x-1}\right), \quad (18)$$

$$Q_1(x) = \frac{x}{2} \ln\left(\frac{x+1}{x-1}\right) - 1 = xQ_0(x) - 1. \quad (19)$$

The quark self energy can be recast in the basis of right and left-hand chiral projection operators as

$$\Sigma(P) = -P_R(A'\not{P} + (B' + C')\not{\psi} + D'\not{b})P_L - P_L(A'\not{P} + (B' - C')\not{\psi} - D'\not{b})P_R. \quad (20)$$

We can re-write the inverse fermion propagator (7) using (20) as

$$S^{*-1}(P) = \not{P} + P_R [A'\not{P} + (B' + C')\not{\psi} + D'\not{b}] P_L + P_L [A'\not{P} + (B' - C')\not{\psi} - D'\not{b}] P_R, \quad (21)$$

which can further be simplified as

$$S^{*-1}(P) = P_R \not{L} P_L + P_L \not{R} P_R. \quad (22)$$

Since  $P_{L,R}\gamma^\mu = \gamma^\mu P_{R,L}$  and  $P_L \not{P} P_L = P_R \not{P} P_R = P_L P_R \not{P} = 0$ ,  $\not{L}$  and  $\not{R}$  are given by

$$\not{L} = (1 + A')\not{P} + (B' + C')\not{\psi} + D'\not{b}, \quad (23)$$

$$\not{R} = (1 + A')\not{P} + (B' - C')\not{\psi} - D'\not{b}. \quad (24)$$

After inverting Eqn. (22), we get the effective quark propagator as

$$S^*(P) = \frac{1}{2} \left[ P_L \frac{\not{L}}{L^2/2} P_R + P_R \frac{\not{R}}{R^2/2} P_L \right], \quad (25)$$

where

$$L^2 = (1 + A')^2 P^2 + 2(1 + A')(B' + C')p_0 - 2D'(1 + A')p_z + (B' + C')^2 - D'^2, \quad (26)$$

$$R^2 = (1 + A')^2 P^2 + 2(1 + A')(B' - C')p_0 + 2D'(1 + A')p_z + (B' - C')^2 - D'^2. \quad (27)$$

Now in order to get the quark thermal mass in weakly magnetized thermal QCD medium, we take the static limit ( $p_0 = 0$ ,  $|\mathbf{p}| \rightarrow 0$ ) of  $L^2/2$  and  $R^2/2$  modes,<sup>1</sup> we get (suppressing the flavor index)

$$\frac{L^2}{2} \Big|_{p_0=0, |\mathbf{p}| \rightarrow 0} = m_T^2 + 4g^2 C_F M^2, \quad (28)$$

$$\frac{R^2}{2} \Big|_{p_0=0, |\mathbf{p}| \rightarrow 0} = m_T^2 - 4g^2 C_F M^2, \quad (29)$$

where,  $m_T$  and  $M$  are as defined in Eqs.(2) and (17), respectively. Here, we can infer that the otherwise degenerate left- and right- handed modes get separated out in presence of weak magnetic field as

$$m_L^2 = m_T^2 + 4g^2 C_F M^2, \quad (30)$$

$$m_R^2 = m_T^2 - 4g^2 C_F M^2. \quad (31)$$

We will use these thermally generated masses in the dispersion relation of the quarks to calculate the Seebeck and Nernst coefficients in the forthcoming sections.

---

<sup>1</sup>We have expanded the Legendre functions appearing in the structure functions in power series of  $\frac{|\mathbf{p}|}{p_0}$  and have considered only upto  $\mathcal{O}(g^2)$

### III Thermoelectric response of an anisotropic QCD medium

QGP produced in relativistic heavy ion collisions can possess a significant temperature gradient between its central and peripheral regions. A temperature-gradient and a finite chemical potential in a conducting medium create the necessary conditions for the Seebeck effect. Charge carriers diffuse from regions of higher temperature to regions of lower temperature. This diffusion of charge carriers constitutes the Seebeck current, which leads to the generation of an electric field. The diffusion ceases when the strength of the created electric field balances the thermodynamic gradient. The magnitude of electric field thus generated per unit temperature gradient in the medium is termed as the Seebeck coefficient and is evaluated in the limit of zero electric current[93, 94]. The Seebeck coefficient is a quantitative estimate of the efficiency of conversion of a temperature gradient into electric field by a conducting medium. The sign of the Seebeck coefficient can be used to determine the sign of majority charge carriers in condensed matter systems, as it is positive for positive charge carriers and negative for negative charge carriers. Upcoming experimental programs such as the Facility for Antiproton and Ion Research (FAIR) in Germany and the Nuclotron-based Ion Collider fAcility (NICA) in Russia, where low-energy heavy ion collisions are expected to create a baryon-rich plasma, could be the perfect environment for the aforementioned thermoelectric phenomenon to manifest.

In the presence of a magnetic field, the charged particles drift perpendicular to their original direction of motion due to the Lorentz force acting on them. This leads to a thermocurrent that is transverse to both the direction of temperature gradient and the external magnetic field. This is called the Nernst effect. Like the Seebeck coefficient, the Nernst coefficient is also calculated at the limit of zero electric current, that is, by enforcing the equilibrium condition. The Nernst coefficient can be defined as the electric field induced in the  $\hat{x}$  ( $\hat{y}$ ) direction per unit temperature gradient in the  $\hat{y}$  ( $\hat{x}$ ) direction, in the presence of a magnetic field pointing in the  $\hat{z}$  direction.

Due to a larger expansion rate of the medium along the longitudinal direction compared to the radial direction, one develops a local momentum anisotropy. This anisotropy can be taken into account by introducing an anisotropy parameter  $\xi$  in the isotropic distribution function. For the case of weak momentum anisotropy ( $\xi < 1$ ) the distribution function of quarks in an anisotropic medium in the presence of a finite quark chemical potential  $\mu$  can be approximated as (suppressing the flavor index) [22].

$$f_a^0(\mathbf{p}; T) = \frac{1}{e^{\beta(\sqrt{p^2 + \xi(\mathbf{p}\cdot\mathbf{n})^2 + m^2} - \mu)} + 1}, \quad (32)$$

which can be expanded in a Taylor series about  $\xi = 0$  (isotropic case) in the following

way:

$$f_a^0 = f^0 - \xi \beta \frac{(\mathbf{p} \cdot \mathbf{n})^2}{2\epsilon} f^0 (1 - f^0), \quad (33)$$

with

$$f^0 = f_a^0(\xi = 0) = \frac{1}{e^{\beta(\sqrt{p^2 + m^2} - \mu)} + 1}, \quad (34)$$

where,  $\beta = 1/T$ . The anisotropy parameter  $\xi$  is defined as

$$\xi = \frac{\langle p_T^2 \rangle}{2 \langle p_L^2 \rangle} - 1, \quad (35)$$

where,  $p_L$  and  $\mathbf{p}_T$  refer to the longitudinal and transverse components of  $\mathbf{p}$ . The 2 in the denominator denotes the fact that there are two transverse directions with respect to any given vector. The condition of isotropy is when  $\langle p_T^2 \rangle = 2 \langle p_L^2 \rangle$ . For  $p_T > 2p_L$ ,  $\xi$  is positive. The aforementioned components are defined with respect to an arbitrary anisotropy direction, denoted by the vector  $\mathbf{n} = (\sin \alpha, 0, \cos \alpha)$ , with  $\alpha$  being the angle between the direction of anisotropy and the  $z$ -axis. This parameter is arbitrary and hence physical quantities should be independent of it. The longitudinal and transverse momentum components are then defined as  $p_L = \mathbf{p} \cdot \mathbf{n}$ ,  $\mathbf{p}_T = \mathbf{p} - \mathbf{n}(\mathbf{p} \cdot \mathbf{n})$ . In spherical polar coordinates,  $\mathbf{p} = (p \sin \theta \cos \phi, p \sin \theta \sin \phi, p \cos \theta)$ , where,  $\theta$  and  $\phi$  are the polar and azimuthal angles, respectively.  $(\mathbf{p} \cdot \mathbf{n})^2 = p^2 c(\theta, \alpha, \phi) = p^2 (\sin^2 \alpha \sin^2 \theta \cos^2 \phi + \cos^2 \alpha \cos^2 \theta + \sin 2\alpha \sin \theta \cos \theta \cos \phi)$ .

### III.A In the absence of magnetic field

In this section, we evaluate the thermoelectric response of the anisotropic QGP medium in the absence of a background magnetic field within the kinetic theory framework. Our starting point is the time evolution of a single particle distribution function, which is given by the relativistic Boltzmann transport equation, which, in the relaxation time approximation reads

$$p \cdot \frac{\partial f_a}{\partial \mathbf{r}} + q \mathbf{E} \cdot \mathbf{p} \frac{\partial f_a}{\partial p^0} + q p_0 \mathbf{E} \cdot \frac{\partial f_a}{\partial \mathbf{p}} = -\frac{p^\mu u_\mu}{\tau} (f_a - f_a^0), \quad (36)$$

where  $f_a = f_a^0 + \delta f_a$ ,  $\delta f$  being the deviation in the equilibrium distribution function due to the electric field produced as a result of thermal gradients in the medium, and  $f_a^0$  is as defined in Eq.(32) with  $m$  as defined in Eq.(1).  $\tau$  is the relaxation time. Once the system is infinitesimally disturbed from equilibrium, it takes on the average an amount of time  $\tau$  to revert to equilibrium. The relaxation time has been calculated for the quarks considering  $2 \rightarrow 2$  scatterings using perturbative QCD as [95]

$$\tau(T) = \frac{1}{5.1 T \alpha_s^2 \log\left(\frac{1}{\alpha_s}\right) [1 + 0.12(2N_f + 1)]}, \quad (37)$$



where  $\alpha_s$  is the running coupling constant (3).

In order to calculate the deviation  $\delta f$ , we assume that the system deviates only infinitesimally away from equilibrium, *i.e.*  $\delta f \ll f^0$ . We then compute the relevant derivatives required to evaluate the left hand side of Eq. (36):

$$\frac{\partial f_a^0}{\partial p} = \frac{\partial f^0}{\partial p} \left[ 1 - \xi \beta \frac{c}{2} \left\{ \frac{p^2}{2\beta\epsilon^2} - \frac{2}{\beta} + \frac{p^2}{\epsilon} - \frac{2p^2}{\epsilon} f^0 \right\} \right] = \frac{\partial f^0}{\partial p} L_1(p, \xi) \quad (38)$$

$$\frac{\partial f_a^0}{\partial \epsilon} = \frac{\partial f^0}{\partial \epsilon} \left[ 1 - \xi \beta \frac{c}{2} \left\{ \frac{p^2}{\epsilon} - \frac{2f^0 p^2}{\epsilon} + \frac{p^2}{\beta\epsilon^2} \right\} \right] = \frac{\partial f^0}{\partial \epsilon} L_2(p, \xi) \quad (39)$$

$$\frac{\partial f_a^0}{\partial r} = \frac{\partial f^0}{\partial r} \left[ 1 - \xi \beta \frac{c}{2} \left\{ \frac{p^2}{\epsilon} - \frac{2f^0 p^2}{\epsilon} - \frac{p^2}{\epsilon(\epsilon - \mu)} \right\} \right] = \frac{\partial f^0}{\partial r} L_3(p, \xi), \quad (40)$$

where,  $\epsilon = \sqrt{p^2 + m^2}$ . As expected, the above derivatives reduce to their isotropic expressions on putting  $\xi = 0$ . We substitute these derivatives in Eq. (36) to get  $\delta f$

$$\begin{aligned} \delta f_a &= -\beta^2 \tau (\epsilon - \mu) f_0 (1 - f_0) \frac{\mathbf{p}}{\epsilon} \cdot \nabla \mathbf{T} L_3(p, \xi) + \tau q \frac{\mathbf{E} \cdot \mathbf{p}}{\epsilon} \beta f_0 (1 - f_0) L_2(p, \xi) \\ &+ \tau q \frac{\mathbf{E} \cdot \mathbf{p}}{\epsilon} \beta f_0 (1 - f_0) L_1(p, \xi). \end{aligned} \quad (41)$$

Similarly, we calculate the deviation  $\delta \bar{f}$  for the anti quarks. This is done by replacing the quark distribution function  $f$  by the anti-quark distribution function  $\bar{f}$  and changing the sign of the chemical potential  $\mu$ .

$$\begin{aligned} \delta \bar{f}_a &= -\beta^2 \tau (\epsilon + \mu) \bar{f}_0 (1 - \bar{f}_0) L_3(p, \xi) \frac{\mathbf{p}}{\epsilon} \cdot \nabla \mathbf{T} + \tau q \frac{\mathbf{E} \cdot \mathbf{p}}{\epsilon} L_2(p, \xi) \beta \bar{f}_0 (1 - \bar{f}_0) \\ &+ \tau \bar{q} \frac{\mathbf{E} \cdot \mathbf{p}}{\epsilon} L_1(p, \xi) \beta \bar{f}_0 (1 - \bar{f}_0), \end{aligned} \quad (42)$$

where, the anti-quark isotropic distribution function is

$$\bar{f}^0 = \frac{1}{e^{\beta(\epsilon + \mu)} + 1}. \quad (43)$$

We consider the temperature gradient to exist in the  $x$ - $y$  plane, *i.e.*

$$\nabla T = \frac{\partial T}{\partial x} \hat{\mathbf{x}} + \frac{\partial T}{\partial y} \hat{\mathbf{y}}. \quad (44)$$

Consequently, the induced electric field is also considered to be planar, *i.e.*,  $\mathbf{E} = E_x \hat{\mathbf{x}} + E_y \hat{\mathbf{y}}$ . The induced four current due to a single quark flavour can be written as

$$J^\mu = g \int \frac{d^3 p}{(2\pi)^3} \frac{p^\mu}{\epsilon} [q \delta f_a + \bar{q} \delta \bar{f}_a], \quad (45)$$

where,  $g$  is the quark degeneracy factor.

Now substituting  $\delta f$  and  $\delta \bar{f}$  in Eq.(45) and putting the induced current to zero in the steady state we get

$$\mathbf{E} = S \nabla T. \quad (46)$$

Here,  $S$  is the *individual* Seebeck coefficient, *i.e.* the Seebeck coefficient of a hypothetical medium consisting of a single quark flavor.

$$S = -\frac{H_1}{H_2} \quad (47)$$

where

$$H_1 = \frac{qg\beta^2}{3} \int \frac{d^3p}{(2\pi)^3} \frac{p^2\tau}{\epsilon^2} \left\{ (\epsilon + \mu)\bar{f}_0(1 - \bar{f}_0)L_3(p, \xi) - (\epsilon - \mu)f_0(1 - f_0)L_3(p, \xi) \right\} \quad (48)$$

$$H_2 = \frac{q^2g\beta}{3} \int \frac{d^3p}{(2\pi)^3} \frac{p^2\tau}{\epsilon^2} \left\{ f_0(1 - f_0)L_1(p, \xi) + \bar{f}_0(1 - \bar{f}_0)L_1(p, \xi) \right\}. \quad (49)$$

To evaluate the Seebeck coefficient of the composite medium, we need to take into account the total current due to multiple quark species. The spatial part of the total 4-current is given by

$$\mathbf{J} = \sum_i q_i g_i \int \frac{d^3p}{(2\pi)^3} \epsilon \mathbf{p} \left[ \delta f_a^i - \overline{\delta f_a^i} \right] \quad (50)$$

Setting the  $x$  and  $y$  components of the above equation to zero yields the following equations:

$$\sum_{i=u,d} \left[ (H_2)_i E_x + (H_1)_i \frac{\partial T}{\partial x} \right] = 0, \quad (51)$$

$$\sum_{i=u,d} \left[ (H_2)_i E_y + (H_1)_i \frac{\partial T}{\partial y} \right] = 0, \quad (52)$$

Solving the above equations and comparing with Eq.(46), we get

$$\begin{pmatrix} E_x \\ E_y \end{pmatrix} = \begin{pmatrix} S_{tot} & 0 \\ 0 & S_{tot} \end{pmatrix} \begin{pmatrix} \frac{\partial T}{\partial x} \\ \frac{\partial T}{\partial y} \end{pmatrix} \quad (53)$$

where, the total Seebeck coefficient  $S_{tot}$  is given by

$$S_{tot} = -\frac{C_1 C_2}{C_2^2}, \quad (54)$$

with

$$C_1 = \sum_{i=u,d} (H_1)_i, \quad C_2 = \sum_{i=u,d} (H_2)_i \quad (55)$$

In the next subsection, we will see how the weak magnetic field in the background modulates the thermoelectric response of the hot QCD medium.

### III.B In the presence of weak magnetic field

The RBTE [Eq.(36)] in 3-vector notation, in the presence of the Lorentz force can be written as

$$\frac{\partial f_a}{\partial t} + \mathbf{v} \cdot \frac{\partial f_a}{\partial \mathbf{r}} + q (\mathbf{E} + \mathbf{v} \times \mathbf{B}) \cdot \frac{\partial f_a}{\partial \mathbf{p}} = -\frac{\delta f_a}{\tau}, \quad (56)$$

In the first approximation, we replace  $f_a$  by  $f_0$  in the L.H.S. above, similar to the  $B = 0$  case. However, we note that the equilibrium distribution function  $f_a^0$  does not contribute to the Lorentz force as  $\frac{\partial f_a^0}{\partial \mathbf{p}} \propto \mathbf{v}$ , hence,  $(\mathbf{v} \times \mathbf{B}) \cdot \frac{\partial f_a^0}{\partial \mathbf{p}} = 0$ . The contribution to the Lorentz force thus comes solely from  $\delta f_a$ . Additionally, we work in the static approximation where, both  $f_a$  and  $f_a^0$  do not depend on time, so that the first term in Eq.(56) drops out. The RBTE thus gets reduced to

$$\mathbf{v} \cdot \frac{\partial f_a^0}{\partial \mathbf{r}} + q \mathbf{E} \cdot \frac{\partial f_a^0}{\partial \mathbf{p}} + q(\mathbf{v} \times \mathbf{B}) \cdot \frac{\partial(\delta f_a)}{\partial \mathbf{p}} = -\frac{\delta f_a}{\tau} \quad (57)$$

As earlier,  $f_a = f_a^0 + \delta f_a$  with  $\delta f_a \ll f_a^0$ . To solve for  $\delta f_a$  we take an ansatz, similar to a trial solution for solving any differential equation[75]:

$$\delta f_a = (\mathbf{p} \cdot \boldsymbol{\Sigma}) \frac{\partial f_a^0}{\partial \epsilon} \quad (58)$$

where,

$$\boldsymbol{\Sigma} = \alpha_1 \mathbf{E} + \alpha_2 \mathbf{b} + \alpha_3 (\mathbf{E} \times \mathbf{b}) + \alpha_4 \nabla \mathbf{T} + \alpha_5 (\nabla \mathbf{T} \times \mathbf{b}) + \alpha_6 (\nabla \mathbf{T} \times \mathbf{E}). \quad (59)$$

Using Eqs.(59) and (58) in Eq.(57), we get,

$$\begin{aligned} & \beta^2 (\epsilon - \mu) f_0 (1 - f_0) L_3(p, \xi) \mathbf{v} \cdot \nabla \mathbf{T} - \beta q f_0 (1 - f_0) L_1(p, \xi) \mathbf{v} \cdot \mathbf{E} - \beta q f_0 (1 - f_0) L_2(p, \xi) \\ & \quad \{-\alpha_1 |B| \mathbf{v} \cdot (\mathbf{E} \times \mathbf{b}) + \alpha_3 |B| \mathbf{v} \cdot \mathbf{E} - \alpha_4 |B| \mathbf{v} \cdot (\nabla \mathbf{T} \times \mathbf{b}) + \alpha_5 |B| \mathbf{v} \cdot \nabla \mathbf{T}\} = \\ & f_0 (1 - f_0) L_2(p, \xi) \frac{\epsilon}{\tau} \{\alpha_1 \mathbf{v} \cdot \mathbf{E} + \alpha_2 \mathbf{v} \cdot \mathbf{b} + \alpha_3 \mathbf{v} \cdot (\mathbf{E} \times \mathbf{b}) + \alpha_4 \mathbf{v} \cdot \nabla \mathbf{T} + \alpha_5 \mathbf{v} \cdot (\nabla \mathbf{T} \times \mathbf{b})\} \quad (60) \end{aligned}$$

Now comparing the coefficients of the same tensor structure of from both sides, we get

$$\frac{\epsilon}{\tau} \alpha_1 L_2(p, \xi) = -\alpha_3 q |B| L_2(p, \xi) - q L_1(p, \xi) \quad (61)$$

$$\frac{\epsilon}{\tau} \alpha_2 L_2(p, \xi) = 0 \quad (62)$$

$$\frac{\epsilon}{\tau} \alpha_3 L_2(p, \xi) = \alpha_1 q |B| L_2(p, \xi) \quad (63)$$

$$\frac{\epsilon}{\tau} \alpha_4 L_2(p, \xi) = \beta (\epsilon - \mu) L_3(p, \xi) - \alpha_5 q |B| L_2(p, \xi) \quad (64)$$

$$\frac{\epsilon}{\tau} \alpha_5 L_2(p, \xi) = \alpha_4 q |B| L_2(p, \xi) \quad (65)$$

We find the values of  $\alpha_1$ ,  $\alpha_2$ ,  $\alpha_3$ ,  $\alpha_4$  and  $\alpha_5$  from the above equations, which come out to be

$$\alpha_1 = -\frac{\tau}{\epsilon} \frac{q}{(1 + \omega_c^2 \tau^2)} \frac{L_1(p, \xi)}{L_2(p, \xi)} \quad (66)$$

$$\alpha_2 = 0 \quad (67)$$

$$\alpha_3 = -\frac{\tau^2}{\epsilon} \frac{\omega_c q}{(1 + \omega_c^2 \tau^2)} \frac{L_1(p, \xi)}{L_2(p, \xi)} \quad (68)$$

$$\alpha_4 = \frac{\tau}{\epsilon} \frac{\beta(\epsilon - \mu)}{(1 + \omega_c^2 \tau^2)} \frac{L_3(p, \xi)}{L_2(p, \xi)} \quad (69)$$

$$\alpha_5 = \frac{\tau^2}{\epsilon} \frac{\omega_c \beta(\epsilon - \mu)}{(1 + \omega_c^2 \tau^2)} \frac{L_3(p, \xi)}{L_2(p, \xi)} \quad (70)$$

$$\delta f = \frac{\tau}{(1 + \omega_c^2 \tau^2)} \mathbf{p} \cdot \left\{ \left( -\frac{q}{\epsilon} \mathbf{E} - \frac{q\tau\omega_c}{\epsilon} (\mathbf{E} \times \mathbf{b}) \right) \frac{L_1(p, \xi)}{L_2(p, \xi)} \right. \quad (71)$$

$$\left. + \left( \frac{\beta(\epsilon - \mu)}{\epsilon} \nabla \mathbf{T} + \frac{\beta\tau\omega_c(\epsilon - \mu)}{\epsilon} (\nabla \mathbf{T} \times \mathbf{b}) \right) \frac{L_3(p, \xi)}{L_2(p, \xi)} \right\} \frac{\partial f^0}{\partial \epsilon} L_2(p, \xi) \quad (72)$$

Similarly, we can compute the deviation in the anti quarks distribution function as

$$\delta \bar{f} = \frac{\tau}{(1 + \omega_c^2 \tau^2)} \mathbf{p} \cdot \left\{ \left( \frac{q}{\epsilon} \mathbf{E} - \frac{q\tau\omega_c}{\epsilon} (\mathbf{E} \times \mathbf{b}) \right) \frac{\bar{L}_1(p, \xi)}{\bar{L}_2(p, \xi)} \right. \quad (73)$$

$$\left. + \left( \frac{\beta(\epsilon + \mu)}{\epsilon} \nabla \mathbf{T} - \frac{\beta\tau\omega_c(\epsilon + \mu)}{\epsilon} (\nabla \mathbf{T} \times \mathbf{b}) \right) \frac{\bar{L}_3(p, \xi)}{\bar{L}_2(p, \xi)} \right\} \frac{\partial \bar{f}^0}{\partial \epsilon} L_2(p, \xi) \quad (74)$$

The  $x$  and  $y$  components of the induced current density can be written as

$$J_x = I_1 E_x + I_2 E_y + I_3 \frac{\partial T}{\partial x} + I_4 \frac{\partial T}{\partial y} \quad (75)$$

$$J_y = -I_2 E_x + I_1 E_y - I_4 \frac{\partial T}{\partial x} + I_3 \frac{\partial T}{\partial y} \quad (76)$$

The electric field components are related to the temperature gradients, Seebeck and Nernst coefficients via a matrix equation

$$\begin{pmatrix} E_x \\ E_y \end{pmatrix} = \begin{pmatrix} S & N|B| \\ -N|B| & S \end{pmatrix} \begin{pmatrix} \frac{\partial T}{\partial x} \\ \frac{\partial T}{\partial y} \end{pmatrix} \quad (77)$$

where

$$I_1 = \frac{q^2 g \beta}{3} \int \frac{d^3 p}{(2\pi)^3} \frac{p^2}{\epsilon^2} \frac{\tau}{(1 + \omega_c^2 \tau^2)} \left\{ f_0(1 - f_0)L_1(p, \xi) + \bar{f}_0(1 - \bar{f}_0)L_1(p, \xi) \right\} \quad (78)$$

$$I_2 = \frac{q^2 g \beta}{3} \int \frac{d^3 p}{(2\pi)^3} \frac{p^2}{\epsilon^2} \frac{\omega_c \tau^2}{(1 + \omega_c^2 \tau^2)} \left\{ f_0(1 - f_0)L_1(p, \xi) - \bar{f}_0(1 - \bar{f}_0)L_1(p, \xi) \right\} \quad (79)$$

$$I_3 = \frac{qg\beta^2}{3} \int \frac{d^3 p}{(2\pi)^3} \frac{p^2}{\epsilon^2} \frac{\tau}{(1 + \omega_c^2 \tau^2)} \left\{ (\epsilon + \mu)\bar{f}_0(1 - \bar{f}_0)L_3(p, \xi) - (\epsilon - \mu)f_0(1 - f_0)L_3(p, \xi) \right\} \quad (80)$$

$$I_4 = \frac{qg\beta^2}{3} \int \frac{d^3 p}{(2\pi)^3} \frac{p^2}{\epsilon^2} \frac{\omega_c \tau^2}{(1 + \omega_c^2 \tau^2)} \left\{ -(\epsilon - \mu)f_0(1 - f_0)L_3(p, \xi) - (\epsilon + \mu)\bar{f}_0(1 - \bar{f}_0)L_3(p, \xi) \right\} \quad (81)$$

In the state of equilibrium, the components of the induced current density along  $x$  and  $y$  direction vanish *i.e.*  $J_x = J_y = 0$ . We can write from Eqns. (75) and (76)

$$I_1 E_x + I_2 E_y + I_3 \frac{\partial T}{\partial x} + I_4 \frac{\partial T}{\partial y} = 0, \quad (82)$$

$$-I_2 E_x + I_1 E_y - I_4 \frac{\partial T}{\partial x} + I_3 \frac{\partial T}{\partial y} = 0, \quad (83)$$

We can further write Eqns (82) and (83) as

$$E_x = \left( -\frac{I_1 I_3 + I_2 I_4}{I_1^2 + I_2^2} \right) \frac{\partial T}{\partial x} + \left( -\frac{I_2 I_3 - I_1 I_4}{I_1^2 + I_2^2} \right) \frac{\partial T}{\partial y}, \quad (84)$$

$$E_y = \left( -\frac{I_1 I_3 + I_2 I_4}{I_1^2 + I_2^2} \right) \frac{\partial T}{\partial y} - \left( -\frac{I_2 I_3 - I_1 I_4}{I_1^2 + I_2^2} \right) \frac{\partial T}{\partial x}, \quad (85)$$

where,

$$S = -\frac{(I_1 I_3 + I_2 I_4)}{I_1^2 + I_2^2}, \quad (86)$$

$$N|B| = \frac{(I_2 I_3 - I_1 I_4)}{I_1^2 + I_2^2}. \quad (87)$$

The integrals  $I_2$  and  $I_4$  vanishes in the absence of the magnetic field. As a result, the Nernst coefficient also vanishes.

In what follows, we will compute the Seebeck and Nernst coefficients for the medium composed of the  $u$  and  $d$  quarks. In the medium The  $x$  and  $y$  components of the induced current in the medium can then be written as the sum of the individual flavour contributions as

$$J_x = \sum_{i=u,d} \left[ (I_1)_i E_x + (I_2)_i E_y + (I_3)_i \frac{\partial T}{\partial x} + (I_4)_i \frac{\partial T}{\partial y} \right], \quad (88)$$

$$J_y = \sum_{i=u,d} \left[ -(I_2)_i E_x + (I_1)_i E_y - (I_4)_i \frac{\partial T}{\partial x} + (I_3)_i \frac{\partial T}{\partial y} \right]. \quad (89)$$

We extract the Seebeck and Nernst coefficients for the QCD medium composed of  $u$  and  $d$  quarks by imposing the equilibrium condition (*i.e.* putting  $J_x = J_y = 0$ ) as

$$S_{tot}^{B'} = -\frac{(K_1 K_3 + K_2 K_4)}{K_1^2 + K_2^2}, \quad (90)$$

$$N|B| = \frac{(K_2 K_3 - K_1 K_4)}{K_1^2 + K_2^2}. \quad (91)$$

where,

$$\begin{aligned} K_1 &= \sum_{i=u,d} (I_1)_i, & K_2 &= \sum_{i=u,d} (I_2)_i, \\ K_3 &= \sum_{i=u,d} (I_3)_i, & K_4 &= \sum_{i=u,d} (I_4)_i. \end{aligned} \quad (92)$$

## IV Results and discussion

We begin with the results obtained at  $B = 0$ , followed by those obtained at finite  $B$ .

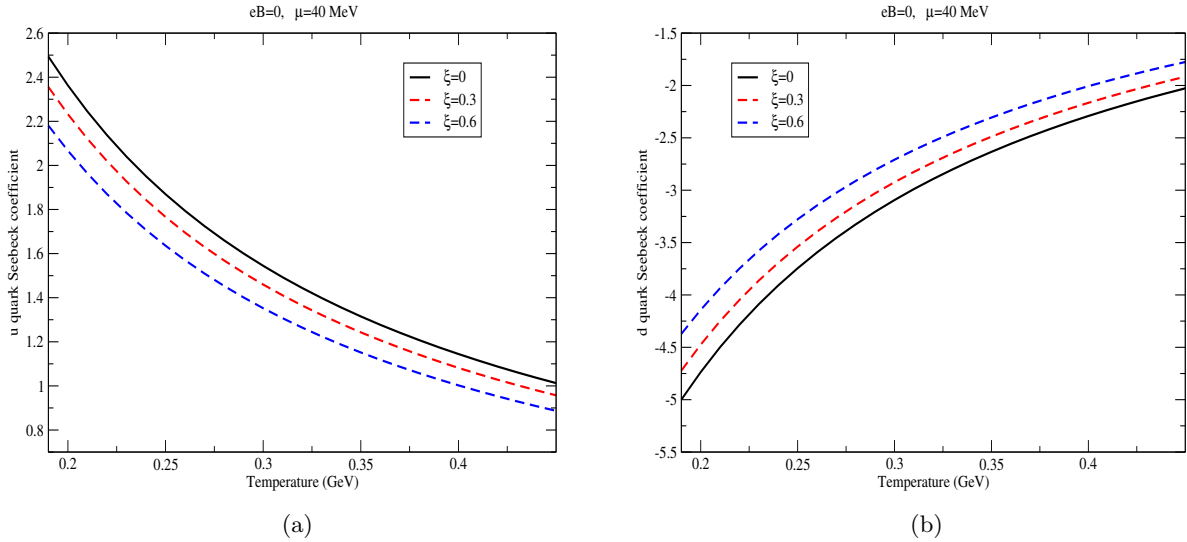


Figure 1: (a) Temperature dependence of  $u$  quark Seebeck coefficient in the absence of  $B$ , at a fixed value of  $\mu$ . (b) Temperature dependence of  $d$  quark Seebeck coefficient in the absence of  $B$ , at a fixed value of  $\mu$ . The different curves correspond to different values of  $\xi$ .

Figs. (1a) and (1b) show the temperature variation of individual seebeck coefficients. That is to say, if the medium were composed exclusively of a single species of quark ( $u$  or

$d$ ), the Seebeck coefficients would vary with temperature as shown in the aforementioned figures. The positively charged  $u$  quark gives rise to a positive Seebeck coefficient, while the same is negative in case of the negatively charged  $d$  quark, which concurs with previous results[74, 76]. Positivity of the Seebeck coefficient indicates that the induced electric field is along the direction of the temperature gradient, whereas a negative value indicates that the induced electric field is in the direction opposite to the direction of the temperature gradient. It should be noted that we have used the convention where the direction of increasing temperature is considered positive. The magnitudes of both the individual Seebeck coefficients ( $S_u$ ,  $S_d$ ) decrease with temperature. Importantly, the magnitudes also decrease with the strength of anisotropy parameter  $\xi$ .  $S_u$  decreases by 5.32% while going from  $\xi = 0$  to  $\xi = 0.3$ , averaged over the entire temperature range. From  $\xi = 0.3$  to  $\xi = 0.6$ , the decrease is 7.11%. Interestingly, the corresponding values for  $S_d$  are identical upto two decimal places.

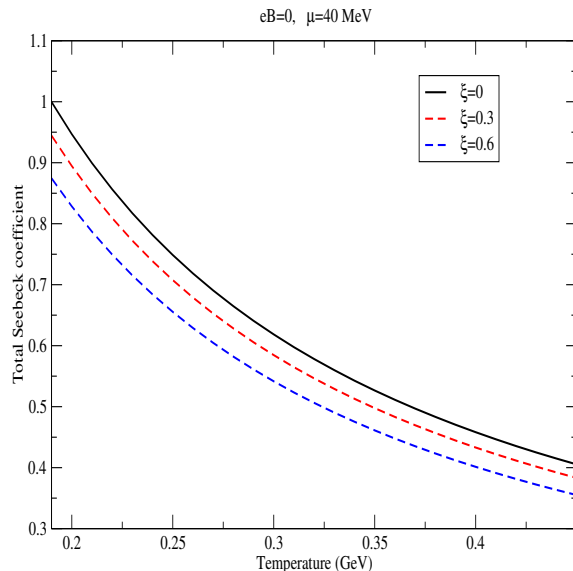


Figure 2: Seebeck coefficient of the composite medium in the absence of  $B$  as a function of temperature.

Fig.(2) shows the Seebeck coefficient of the composite medium composed of  $u$  and  $d$  quarks-the total Seebeck coefficient ( $S_{\text{tot}}$ ), as a function of temperature.  $S_{\text{tot}}$  is positive and decreases with temperature. So, the induced electric field points in along the temperature gradient. Also, it is to be noted that even though the magnitude of  $d$  quark Seebeck coefficient is larger than that of the  $u$  quark at a given temperature, the total coefficient is positive. This reflects the fact that a  $u$  quark carries double the electric charge than a  $d$  quark. Again, a finite anisotropy decreases the magnitude of  $S_{\text{tot}}$ . It decreases by 5.31% in going from  $\xi = 0$  to  $\xi = 0.3$ , and by 7.11% when  $\xi$  changes from 0.3 to 0.6. The decrease in the magnitude of transport coefficients with anisotropy has been observed earlier[45].

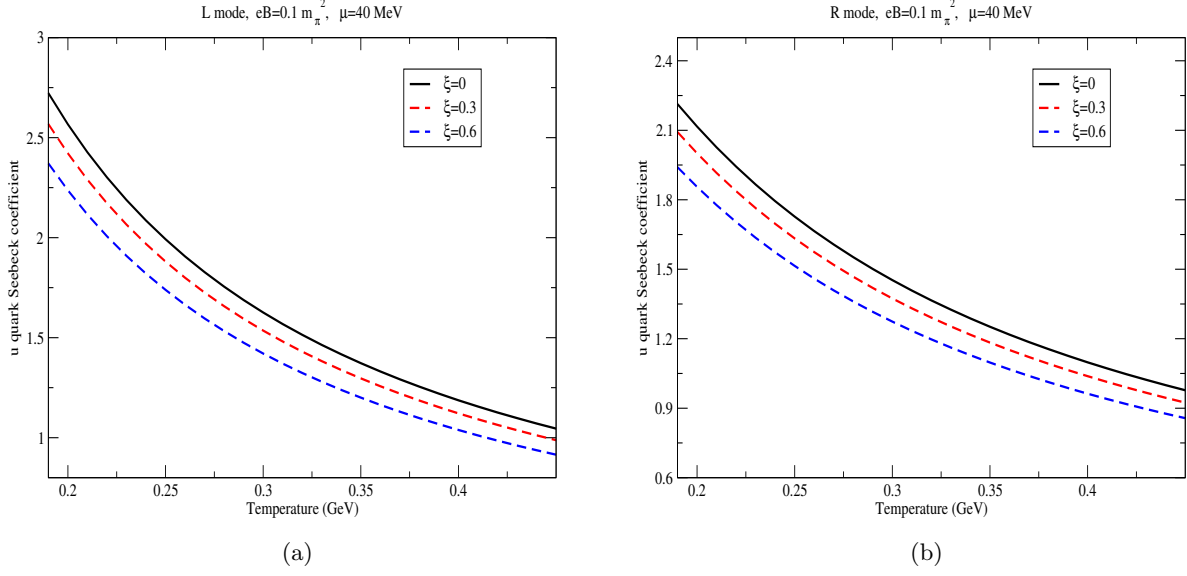


Figure 3: (a) Temperature dependence of  $u$  quark  $L$  mode Seebeck coefficient at fixed values of  $eB$  and  $\mu$ . (b) Temperature dependence of  $u$  quark  $R$  mode Seebeck coefficient at fixed values of  $eB$  and  $\mu$ . The different curves correspond to different values of  $\xi$

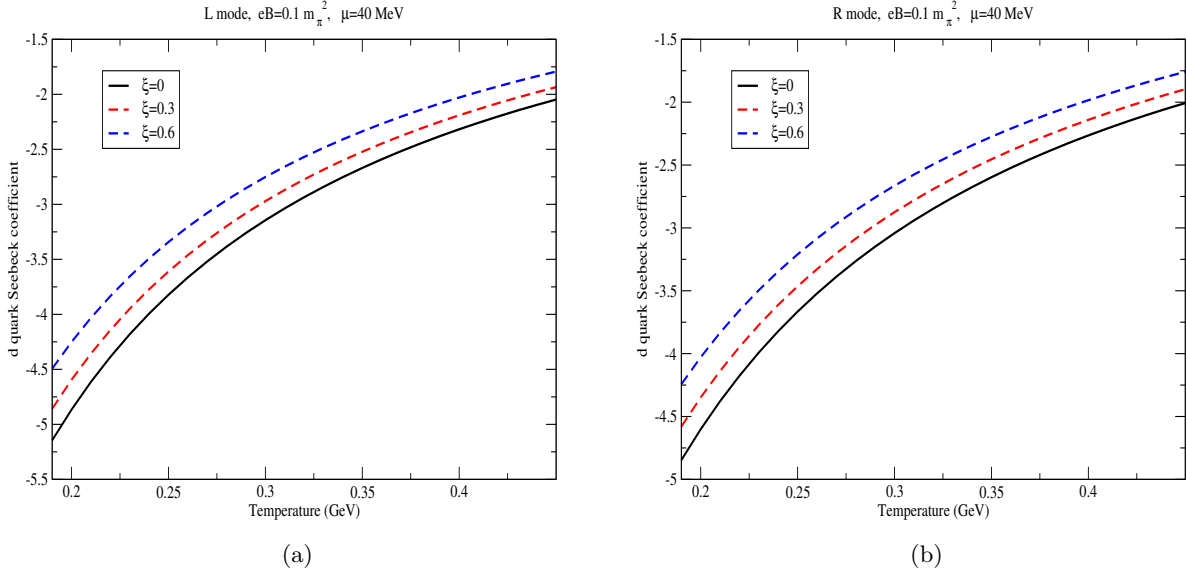


Figure 4: (a) Temperature dependence of  $d$  quark  $L$  mode Seebeck coefficient at fixed values of  $eB$  and  $\mu$ . (b) Temperature dependence of  $d$  quark  $R$  mode Seebeck coefficient at fixed values of  $eB$  and  $\mu$ . The different curves correspond to different values of  $\xi$ .

Figures (3) and (4) show the variation with temperature of  $u$  quark and  $d$  quark Seebeck coefficients, respectively. The coefficient is positive for positively charged  $u$  quark and negative for the negatively charged  $d$  quark, which is along expected lines. As can be seen from the figures, the coefficient magnitudes are decreasing functions of temperature.



One can also see the effect of anisotropy on the coefficient magnitudes. Compared to the isotropic ( $\xi = 0$ ) result, the anisotropic medium leads to a lesser value of the Seebeck coefficient magnitude for a particular value of temperature and magnetic field. Also, with the increase in the extent of anisotropy, the coefficient magnitude decreases. Comparing the graphs for the  $L$  and  $R$  modes shows that the Seebeck coefficient magnitudes for the  $R$  mode are slightly smaller than its  $L$  mode counterpart. This is due to the smaller effective mass of the  $R$  mode compared to the  $L$  mode at the same values of temperature and magnetic field. Specifically, the difference between the magnitudes of the  $L$  and  $R$  modes is greatest at lower temperatures and decreases as the temperature rises. We can take the average in the entire temperature range and define an average percentage change corresponding to each value of  $\xi$ . We found that the percentage decrease in the  $u$  quark coefficient magnitude as one goes from the  $L$  mode to the  $R$  mode is  $\sim 9.95\%$  for  $\xi = 0$ ,  $\sim 9.86\%$  for  $\xi = 0.3$  and  $\sim 9.68\%$  for  $\xi = 0.6$ . This shows that as the strength of anisotropy increases, the difference between the  $L$  and  $R$  magnitudes decreases. Taking the mean of the three values corresponding to the three  $\xi$  values, we arrive at a mean percentage decrease value of  $\sim 9.83\%$ . Interestingly, for the  $d$  quark Seebeck coefficient, these values are  $\sim 3.06\%$  for  $\xi = 0$ ,  $\sim 3.03\%$  for  $\xi = 0.3$  and  $\sim 2.97\%$  for  $\xi = 0.6$ . So, the effect of the difference in  $L$  and  $R$  mode quasiparticle masses is suppressed for the  $d$  quark Seebeck coefficient compared to the  $u$  quark result.

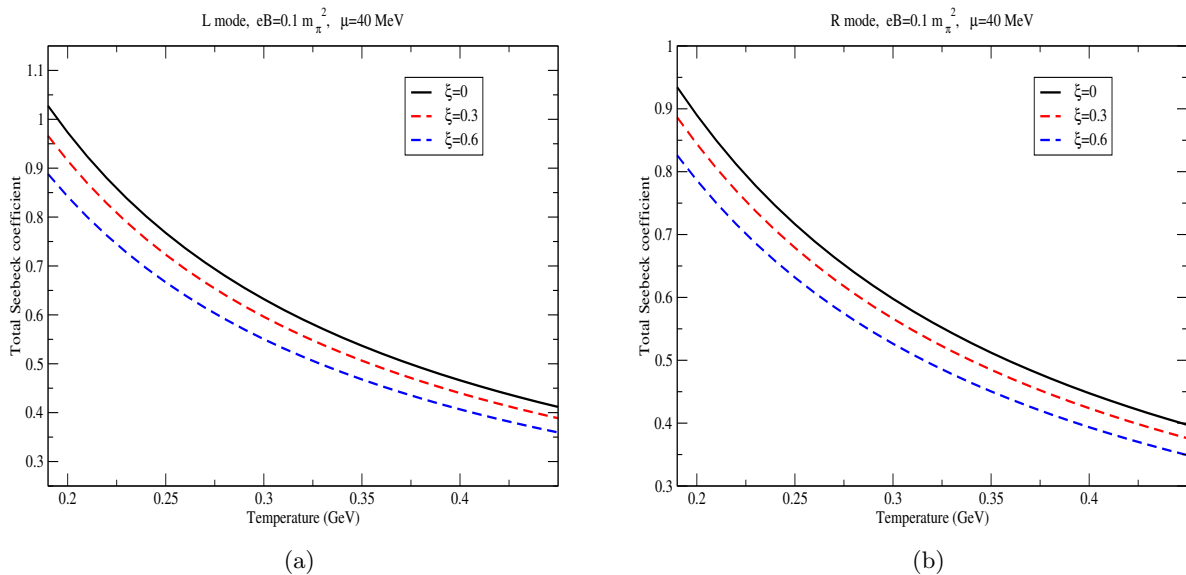


Figure 5: (a) Variation of total Seebeck coefficient of the medium ( $L$  mode) with temperature at fixed values of  $eB$  and  $\mu$ . (b) Variation of total Seebeck coefficient of the medium ( $R$  mode) with temperature at fixed values of  $eB$  and  $\mu$ . The different curves correspond to different values of  $\xi$ .

Figures (5a) and (5b) show the temperature dependence of Seebeck coefficient of the

composite medium composed of  $u$  and  $d$  quarks. The total Seebeck coefficient is positive, which means that the induced electric field of the medium points in the direction of increasing temperature. The coefficient magnitude decreases with temperature and also decreases with increase in the anisotropy parameter  $\xi$ . As in the case of the individual coefficients, the  $R$  mode Seebeck coefficient magnitude is slightly smaller than that of the  $L$  mode, which again can be attributed to the smaller effective mass of the  $R$  mode quasi-quark. The average (over  $T$  and  $\xi$  both) percentage decrease as one goes from the  $L$  mode to the  $R$  mode composite Seebeck coefficient is  $\sim 4.61\%$ . Here also, the percentage difference between the two modes decreases with increasing anisotropy strength. Thus, anisotropic expansion of the medium hinders the ability of a thermal QCD medium to convert a temperature gradient to electric field.

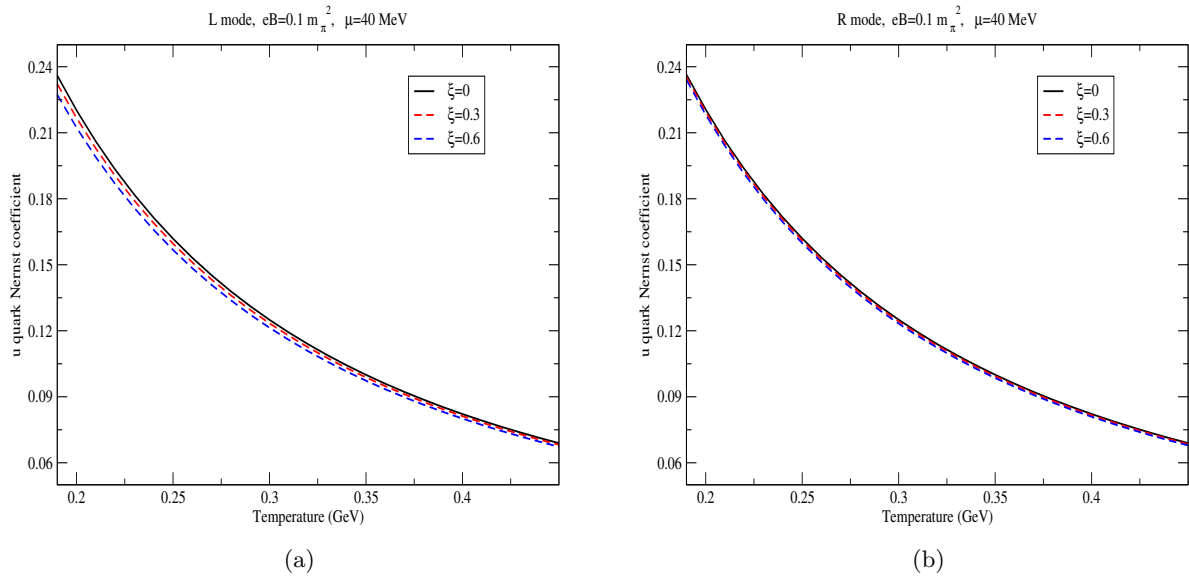


Figure 6: (a) Variation of  $u$  quark  $L$  mode Nernst coefficient with temperature at fixed values of  $eB$  and  $\mu$ . (b) Variation of  $u$  quark  $R$  mode Nernst coefficient with temperature at fixed values of  $eB$  and  $\mu$ . The different curves correspond to different values of  $\xi$ .

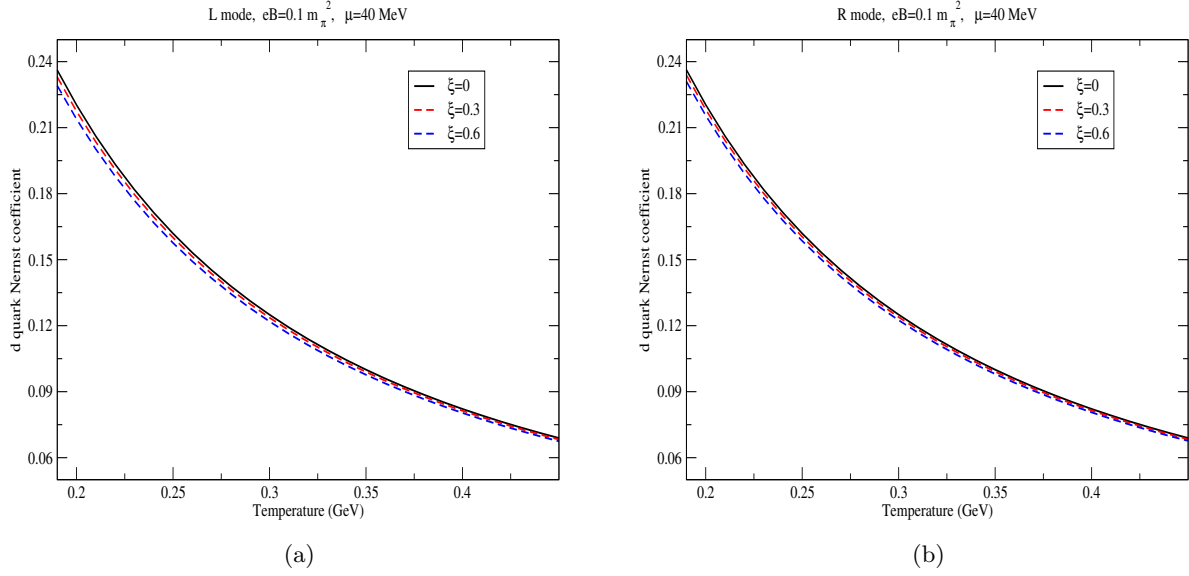


Figure 7: (a) Variation of  $d$  quark  $L$  mode Nernst coefficient with temperature at fixed values of  $eB$  and  $\mu$ . (b) Variation of  $d$  quark  $R$  mode Nernst coefficient with temperature at fixed values of  $eB$  and  $\mu$ . The different curves correspond to different values of  $\xi$ .

Figures (6a) and (6b) show the variation with temperature, of the Nernst coefficient corresponding to the  $L$  and  $R$  modes, respectively, of a medium composed exclusively of  $u$  quarks. Similar to the Seebeck coefficient, the Nernst coefficient magnitude decreases with temperature and also decreases with the value of the anisotropy parameter  $\xi$ . Comparison between the graphs corresponding to the  $L$  and  $R$  modes reveals that  $R$  mode magnitudes are slightly more than that of the  $L$  mode. This trend is opposite to the individual Seebeck coefficient case where  $R$  mode magnitudes were less than their  $L$  mode counterparts. Also, the extent of difference between the two modes is much smaller compared to the Seebeck coefficient case. Specifically, for the  $u$  quark nernst coefficient, the temperature averaged percentage decrease as one goes from  $R$  mode to  $L$  mode is 0.051% for  $\xi = 0$ ,  $\sim 0.65\%$  for  $\xi = 0.3$  and  $\sim 1.43\%$  for  $\xi = 0.6$ . Taking the mean of the values corresponding to the different  $\xi$  values gives us an average value of 0.71%. Compared to the  $u$  quark Seebeck coefficient, these values are almost an order of magnitude smaller. Also, unlike in the case of the Seebeck coefficients, the percentage change between the  $L$  and  $R$  mode increases sharply with increase in the strength of anisotropy,

The  $d$  quark Nernst coefficients corresponding to the  $L$  and  $R$  modes shown in Figs.(7a) and (7b) respectively show that the magnitudes of Nernst coefficients corresponding to both the modes decreases with temperature. Also, the magnitudes decrease with increase in the degree of anisotropy, parameterized by the value of  $\xi$ . Similar to the  $u$  quark Nernst coefficient, the  $L$  mode absolute values of  $d$  quark Nernst coefficients are smaller than their  $R$  mode counterparts; the averaged (over  $T$ ) percentage decrease being 0.015% for  $\xi = 0$ ,

$\sim 0.192\%$  for  $\xi = 0.3$  and  $\sim 0.422\%$  for  $\xi = 0.6$ . Averaging also over the different  $\xi$  values yields a mean percentage decrease value of  $0.21\%$ . This trend is similar to the individual Seebeck coefficient case where the percentage changes for  $d$  quark Seebeck coefficient was much smaller than that for the  $u$  quark. Also from the magnitudes of the individual Seebeck and Nernst coefficients (both  $u$  and  $d$  quarks), it can be seen that magnitudes of the Nernst coefficients are  $\sim 1$  order of magnitude smaller.

The major point of difference with the Seebeck coefficient, however, is that the Nernst coefficient for both  $u$  and  $d$  quarks is positive. To understand this, let us consider positively charged quarks moving in the  $+\hat{x}$  direction under the influence of a temperature gradient. On application of a magnetic field in the  $\hat{z}$  direction, the Lorentz force will cause them to drift in the  $-\hat{y}$  direction. This will result in an induced electric field in the  $+\hat{y}$  direction. If the electric charge of the quarks were negative instead, they would drift towards the  $+\hat{y}$  direction and pile up there. This would again lead to an induced electric field in the  $+\hat{y}$  direction. Thus, the direction of the induced field does not depend on the sign of the electric charge of the quark, unlike in the case of Seebeck coefficient, resulting in positive Nernst coefficients for both  $u$  and  $d$  quarks.

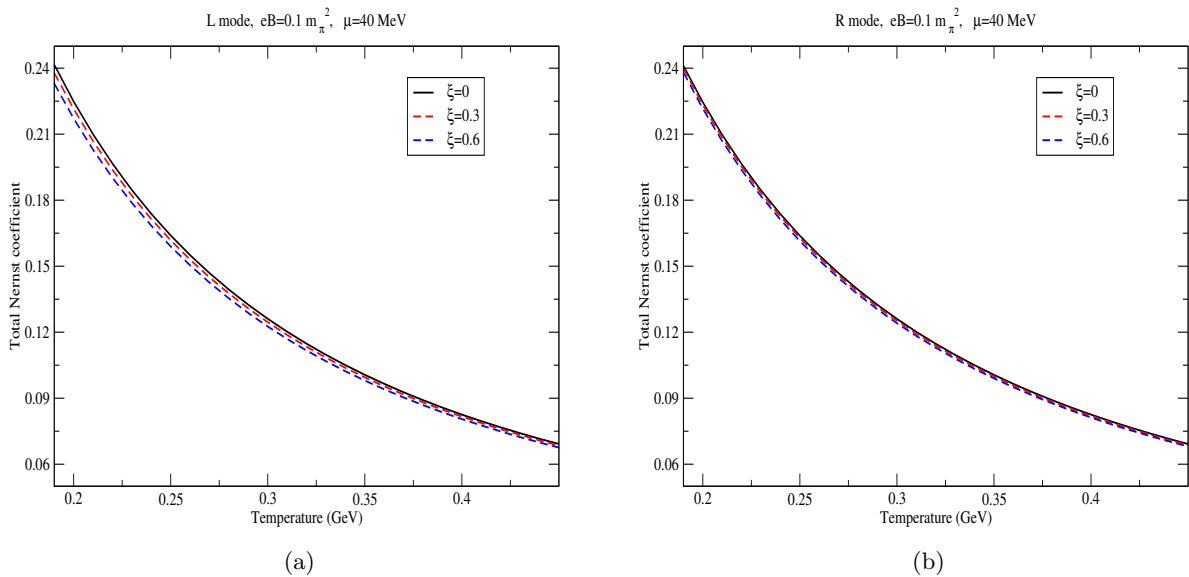


Figure 8: (a) Variation of total Nernst coefficient of the medium ( $L$  mode) with temperature at fixed values of  $eB$  and  $\mu$ . (b) Variation of total Nernst coefficient of the medium ( $R$  mode) with temperature at fixed values of  $eB$  and  $\mu$ . The different curves correspond to different values of  $\xi$ .

Figures (8a) and (8b) show the temperature variation of the Nernst coefficients of the composite medium corresponding to  $L$  mode quasiparticles and  $R$  mode quasiparticles, respectively. The total Nernst coefficient of the medium is positive, and is a decreasing function of temperature. Like its Seebeck counterpart, its magnitude decreases with the strength of anisotropy. Compared to the individual Nernst coefficient magnitudes, the

total Nernst coefficient magnitudes are an order of magnitude smaller. Also, compared to the total Seebeck coefficient, its values are an order of magnitude smaller. This suggests that the Nernst effect in a weakly magnetized thermal QCD medium is a weaker effect compared to the Seebeck effect. Just as in the case of the individual Nernst coefficients, the  $L$  mode values of the total Nernst coefficient are slightly smaller in magnitude than their  $R$  mode counterparts; the averaged (over  $T$ ) percentage decrease being 0.04% for  $\xi = 0$ ,  $\sim 0.47\%$  for  $\xi = 0.3$  and  $\sim 1.14\%$  for  $\xi = 0.6$ . The mean of the three values corresponding to different  $\xi$  is 0.55%. Interestingly, these numbers are  $\sim$  an order of magnitude bigger than corresponding numbers for the individual Nernst coefficients, and an order of magnitude smaller than the corresponding values for the total Seebeck coefficient. Such a drastic change in going from the individual to the total coefficients was not observed for the Seebeck coefficient. Thus, the sensitivity to the mass difference between the  $L$  and  $R$  modes of quarks is much amplified for the composite medium, compared to a single flavor medium.

## V Conclusion

We have estimated the thermoelectric response of a deconfined hot QCD medium in the presence of a weak external magnetic field, taking into account the anisotropic expansion of the QGP fireball. The strength of the response, *i.e.* the ability to convert a temperature gradient into an electric field, is quantified by two coefficients, *viz.* Seebeck coefficient and Nernst coefficient. We have calculated the individual as well as the total response coefficients of the medium and checked their variation with temperature and anisotropy strength. We have presented results both in the absence and presence of a background magnetic field  $B$ . Our plots for finite  $B$  have been generated for a constant background magnetic field of strength  $eB = 0.1 m_\pi^2$ , and a constant chemical potential  $\mu = 40 MeV$ . Because of the lifting of mass degeneracy between the left-handed ( $L$ ) and right-handed ( $R$ ) chiral quark modes, we have shown each result for the two modes separately. We have found that the magnitudes of both the individual as well as the total coefficients—both Seebeck and Nernst, are decreasing functions of temperature, and decreasing functions of anisotropy strength, characterized by the anisotropy parameter  $\xi$ . It is important to note that the Seebeck coefficient vanishes for  $\mu = 0$  irrespective of the magnetic field strength, and the Nernst coefficient vanishes for  $|\mathbf{B}| = 0$ , irrespective of the value of  $\mu$ . We have analysed the sensitivity to the  $L$  and  $R$  modes, *i.e.* to the difference in quasiparticle effective masses of the coefficient magnitudes; both for individual and total. To that end we have calculated the average percentage change in the coefficient magnitude as one goes from the  $L$  mode to the  $R$  mode or vice versa. For the Seebeck coefficient, the average (over  $T$  and  $\xi$ ) percentage change for the  $u$  quark is  $\sim 9.83\%$ , whereas for the  $d$

quark, it is  $\sim 3.02\%$ . This shows that the  $d$  quark Seebeck coefficient is comparatively less sensitive to differences in quasiparticle masses. For the total Seebeck coefficient, the average percentage change in going from the  $L$  mode to the  $R$  mode is  $\sim 4.61\%$ , which is in between the values for the individual coefficients.

Certain differences arise in the case of Nernst coefficient. Firstly, for both the individual and total Nernst coefficients, the absolute values of the  $R$  mode coefficients are greater than that of the  $L$  mode. This is opposite to the case of Seebeck coefficients. The average percentage change in going from the  $R$  mode to the  $L$  mode in case of  $u$  quark Nernst coefficient is  $\sim 0.71\%$ ; for the  $d$  quark Nernst coefficient, this value is  $\sim 0.21\%$ . Compared to their Seebeck counterparts, these numbers are an order of magnitudes smaller, indicating that the individual Nernst coefficients are comparatively much less sensitive to the change in quasiparticle modes. A major difference between the individual Nernst and Seebeck coefficients is that while positively (negatively) charged quarks lead to positive (negative) Seebeck coefficients, the individual Nernst coefficients are independent of the electric charge of the quark. For the case of the total Nernst coefficient, the average percentage decrease from  $R$  to  $L$  modes is  $\sim 0.55\%$ . The absolute values of both the individual and total Nernst coefficients are about 1 order of magnitude smaller than their Seebeck counterparts, which shows that the Nernst effect is a weaker response than the Seebeck effect.

## References

- [1] E. V. Shuryak, *Phys. Lett. A* **78**, 1 (1978).
- [2] J. I. Kapusta, P. Lichard, and D. Seibert, *Phys. Rev. D* **44**, 2774 (1991).
- [3] J. P. Blaizot and J. Y. Ollitrault, *Phys. Rev. Lett.* **77**, 1703 (1996).
- [4] H. Satz, *Nucl. Phys. A* **783**, 249 (2007).
- [5] R. Rapp, D. Blaschke, and P. Crochet, *Prog. Part. Nucl. Phys.* **65**, 209 (2010).
- [6] R. S. Bhalerao and J. Y. Ollitrault, *Phys. Lett. B* **641**, 260 (2006).
- [7] S. A. Voloshin, A. M. Poskanzer, A. Tang, and G. Wang, *Phys. Lett. B* **659**, 537 (2008).
- [8] X. N. Wang and M. Gyulassy, *Phys. Rev. Lett.* **68**, 1480 (1992).
- [9] K. Adcox et al., *Phys. Rev. Lett.* **88**, 022301 (2001).
- [10] S. Chatrchyan et al., *Phys. Rev. C* **84**, 024906 (2011).
- [11] I. Arsene et al., BRAHMS Collaboration, *Nucl. Phys. A* **757**, 1-27 (2005).

- [12] J. Adams et al., STAR Collaboration, *Nucl. Phys. A* **757**, 102-183 (2005).
- [13] K. Adcox et al., PHENIX Collaboration, *Nucl. Phys. A* **757**, 184-283 (2005).
- [14] F. Carminati et al., ALICE Collaboration, *J. Phys. G: Nucl. Part. Phys.* **30**, 1517 (2004).
- [15] B. Alessandro et al., ALICE Collaboration, *J. Phys. G: Nucl. Part. Phys.* **32**, 1295 (2006).
- [16] Y. Aoki, Z. Fodor, S. D. Katz and K. K. Szabo, *Phys. Lett. B* **643**, 46 (2006).
- [17] S. Borsanyi *et al.* *JHEP* **1009**, 073 (2010).
- [18] S. Borsanyi *et al.*, *Phys. Rev. D* **92**, 014505 (2015).
- [19] H. T. Ding, F. Karsch and S. Mukherjee, *Int. J. Mod. Phys E* **24**, 1530007 (2015).
- [20] S. Hands, *Nucl. Phys. B* **106-107** (2002).
- [21] M. G. Alford, *Nucl. Phys. Proc. Suppl.* **117**, 65 (2003).
- [22] P. Romatschke and M. Strickland, *Phys. Rev. D* **68**, 036004 (2003).
- [23] P. Romatschke and M. Strickland, *Phys. Rev. D* **70**, 116006 (2004).
- [24] M. E. Carrington, K. Deja, and S. Mrówczyński, *Phys. Rev. C* **90**, 034913 (2014).
- [25] B. Schenke and M. Strickland, *Phys. Rev. D* **74**, 065004 (2006).
- [26] S. Mrówczyński and M. H. Thoma, *Phys. Rev. D* **62**, 036011 (2000).
- [27] J. Randrup and S. Mrówczyński, *Phys. Rev. C* **68**, 034909 (2003).
- [28] S. Mrówczyński, B. Schenke, and M. Strickland, *Phys. Rep.* **682**, 1 (2017).
- [29] B. Schenke and M. Strickland, *Phys. Rev. D* **76**, 025023 (2007).
- [30] L. Bhattacharya, R. Ryblewski, and M. Strickland, *Phys. Rev. D* **93**, 065005 (2016).
- [31] M. Nopoush, Y. Guo, and M. Strickland, *J. High Energy Phys.* **09** (2017) 063.
- [32] B. Krouppa and M. Strickland, *Universe* **2**, 16 (2016).
- [33] B. S. Kasmaei and M. Strickland *Phys. Rev. D* **97**, 054022 (2018)
- [34] W. Florkowski and R. Ryblewski, *Phys. Rev. C* **83**, 034907 (2011).
- [35] M. Martinez and M. Strickland, *Nucl. Phys. A* **848**, 183 (2010).
- [36] M. Alqahtani, M. Nopoush, R. Ryblewski, and M. Strickland, *Phys. Rev. C* **96**, 044910 (2017).

- [37] M. Alqahtani, M. Nopoush, and M. Strickland, *Progress in Particle and Nuclear Physics* **101**, 204-208 (2018).
- [38] M. Alqahtani, M. Nopoush, R. Ryblewski, and M. Strickland, *Phys. Rev. Lett.* **119**, 042301 (2017).
- [39] W. Florkowski, E. Maksymiuk, R. Ryblewski, and M. Strickland, *Phys. Rev. C* **89**, 054908 (2014).
- [40] M. Nopoush, R. Ryblewski, and M. Strickland, *Phys. Rev. C* **90**, 014908 (2014).
- [41] L. Tinti, R. Ryblewski, W. Florkowski, and M. Strickland, *Nucl. Phys. A* **946**, 29 (2016).
- [42] M. Strickland, M. Nopoush, and R. Ryblewski, *Nucl. Phys. A* **956**, 268 (2016).
- [43] M. Strickland, J. Noronha, and G. Denicol, *Phys. Rev. D* **97**, 036020 (2018).
- [44] M. Strickland, *J. High Energy Phys.* **12** (2018) 128.
- [45] S. Rath and B. K. Patra, *Phys. Rev. D* **100**, 016009 (2019)
- [46] A. Kumar, M. Kurian, S. K. Das and V. Chandra *Phys. Rev. C* **105**, 054903 (2022)
- [47] K. Tuchin, *Adv.High Energy Phys.* , 490495 (2013).
- [48] V. Skokov, A. Illarionov, and V. Toneev, *Int. J. Mod. Phys. A* **24**, 5925 (2009).
- [49] K. Tuchin, *Phys. Rev. C* **82**, 034904 (2010).
- [50] K. Tuchin, *Phys. Rev. C* **83**, 017901 (2011).
- [51] R. Marty, E. Bratkovskaya, W. Cassing, J. Aichelin and H. Berrehrach, *Phys. Rev. C* **88**, 045204 (2013).
- [52] H.-T. Ding, A. Francis, O. Kaczmarek, F. Karsch, E. Laermann, and W. Soeldner, *Phys. Rev. D* **83**, 034504 (2011).
- [53] S. Gupta, *Phys. Lett. B* **597**, 57–62 (2004).
- [54] A. Amato, G. Aarts, C. Allton, P. Giudice, S. Hands, and J.-I. Skullerud, *Phys. Rev. Lett.* **111** no. 17, 172001 (2013).
- [55] G. Aarts, C. Allton, J. Foley, S. Hands, and S. Kim, *Phys. Rev. Lett.* **99**, 022002 (2007).
- [56] A. Puglisi, S. Plumari, and V. Greco, *Phys. Rev. D* **90** (2014) 114009.
- [57] M. Greif, I. Bouras, C. Greiner, and Z. Xu, *Phys. Rev. D* **90** (2014) no. 9, 094014.



- [58] K. Hattori, X. G. Huang, D. H. Rischke, and D. Satow, *Phys. Rev. D* **96**, 094009 (2017).
- [59] D. E. Kharzeev, L. D. McLerran, and H. J. Warringa, *Nucl.Phys. A* **803**, 227 (2008).
- [60] K. Fukushima, D. E. Kharzeev, and H. J. Warringa, *Phys. Rev. D* **78**, 074033 (2008).
- [61] D. E. Kharzeev, *Ann. Phys. (Amsterdam)* **325**, 205 (2010).
- [62] I. A. Shovkovy, *Lect. Notes Phys.* **871**, 13 (2013).
- [63] D. E. Kharzeev and H. U. Yee, *Phys. Rev. D* **83**, 085007 (2011).
- [64] V. Braguta, M. N. Chernodub, V. A. Goy, K. Landsteiner, A. V. Molochkov, and M. I. Polikarpov, *Phys. Rev. D* **89**, 074510 (2014).
- [65] M. N. Chernodub, A. Cortijo, A. G. Grushin, K. Landsteiner, and M. A. H. Vozmediano, *Phys. Rev. B* **89**, 081407 (2014).
- [66] A. Das, A. Bandyopadhyay, P. K. Roy, and M. G. Mustafa, *Phys. Rev. D* **97**, 034024 (2018).
- [67] P. Panday and B. K. Patra, *Phys. Rev. D* **105**, 116009
- [68] A. Das, H. Mishra, and R. K. Mohapatra, *Phys. Rev. D* **101**, 034027 (2020).
- [69] L. Thakur and P. K. Srivastava, *Phys. Rev. D* **100**, 076016 (2019).
- [70] B. Feng, *Phys. Rev. D* **96**, 036009 (2017).
- [71] S. Rath and S. Dash, *Eur. Phys. J. C* **82**, 797 (2022).
- [72] A. Shaikh, S. Rath, S. Dash and B. Panda, [arXiv:2210.15388](https://arxiv.org/abs/2210.15388)
- [73] B. Schenke, P. Tribedy, and R. Venugopalan, *Phys. Rev. Lett.* **108**, 252301 (2012).
- [74] J. R. Bhatt, A. Das, and H. Mishra *Phys. Rev. D* **99**, 014015 (2018).
- [75] A. Das, H. Mishra, and R. K. Mohapatra, *Phys. Rev. D* **102**, 014030 (2020).
- [76] D. Dey and B. K. Patra, *Phys. Rev. D* **102**, 096011 (2020).
- [77] D. Dey and B. K. Patra, *Phys. Rev. D* **104**, 076021 (2021)
- [78] M. Kurian, *Phys. Rev. D* **103**, 054024 (2021).
- [79] H. Zhang, J. Kang, and B. Zhang, *Eur. Phys. J. C* **81**, 623 (2021).
- [80] S. A. Khan and B. K. Patra, [arXiv:2211.10779](https://arxiv.org/abs/2211.10779)
- [81] K. Fukushima, *Phys. Lett. B* **591**, 277 (2004).

- [82] S. K. Ghosh, T. K. Mukherjee, M. G. Mustafa, and R. Ray, *Phys. Rev. D* **73**, 114007 (2006).
- [83] H. Abuki and K. Fukushima, *Phys. Lett. B* **676**, 57 (2009).
- [84] H. M. Tsai, and B. Muller, *J. Phys. G* **36**, 075101 (2009).
- [85] V. Chandra, R. Kumar and V Ravishankar, *Phys. Rev. C*, **76**, 054909 (2007).
- [86] N. Su and K. Tywoniuk, *Phys. Rev. Lett.* **114**, 161601 (2015).
- [87] W. Florkowski, R. Ryblewski, N. Su, and K. Tywoniuk, *Phys. Rev. C* **94**, 044904 (2016).
- [88] A. Jaiswal and N. Haque, *Phys. Lett. B* **811**, 135936 (2020).
- [89] V. M. Bannur, *J. High Energy Phys.* **09** (2007) 046.
- [90] E. Braaten and R. D. Pisarski, *Phys. Rev. D* **45**, R1827 (1992).
- [91] A. Peshier, B. Kämpfer, and G. Soff, *Phys. Rev. D* **66**, 094003 (2002).
- [92] A. Ayala, C. A. Dominguez, S. Hernandez-Ortiz, L. A. Hernandez, M. Loewe, D. Manreza Paret, and R. Zamora, *Phys. Rev. D* **98**, 031501(R) (2018).
- [93] H. B. Callen, *Thermodynamics* (Wiley, New York, 1960).
- [94] T. J. Scheidemantel, C. Ambrosch-Draxi, T. Thonhauser, J. V. Badding, and J. O. Sofo, *Phys. Rev. B* **68**, 125210 (2003).
- [95] A. Hosoya and K. Kajantie, *Nucl. Phys. B***250**, 666 (1985).